Microporous polyphenylenes with tunable pore size for hydrogen storage†

Shengwen Yuan,[a] Brian Dorney,[a] Desiree White,[a] Scott Kirklin,[a] Peter Zapol,[ab] Luping Yu*[c] and Di-Jia Liu*[a]

Received 5th March 2010, Accepted 21st April 2010
First published as an Advance Article on the web 26th May 2010
DOI: 10.1039/c0cc00235f

A series of highly porous polymers with similar BET surface areas of higher than 1000 m^2 g^{-1} but tunable pore ranging from 0.7 nm to 0.9 nm were synthesized through facile ethynyl trimerization reaction to demonstrate the surface property-hydrogen adsorption relationship.

Microporous organic polymers exhibit unique properties of large surface areas, low skeleton density and high chemical stabilities that have applications in gas storage and separation.[1–9] Recently, several types of chemical reactions have been used to develop various cross-linked porous organic polymers, such as dioxane formation for polymers of intrinsic microporosity (PIMs),[1] palladium catalyzed Sonogashira-Hagihara cross-coupling for poly(aryleneethynylene) microporous polymers,[2] Friedel–Crafts reaction for hypercrosslinked polymers,[3,9] oxidative coupling of thiophenes,[4,6b] trimerization of ethynyl groups,[4] amide or imide formation,[6a,d] reversible imine formation,[7] and homocoupling of aromatic bromides.[8] The flexibility of rational design in molecular structures is a major advantage in producing porous polymers with high surface area and narrow pore size distribution. This can be achieved by designing monomers with targeted structures and functional groups for polymerization under proper reaction conditions. Since the pore size affects the heat of adsorption and diffusion kinetics through close interaction between adsorbent and adsorbate, materials with high specific surface area (SSA) and narrow pore diameter (PD) are highly desirable for gas adsorption and separation. It was suggested that the preferred pore size should be slightly higher than the adsorbate's van der Waals dimension[9b] at 0.6 nm to 0.9 nm in the case of hydrogen.

Although most porous polymers are amorphous, Cooper and coworkers have demonstrated the feasibility of systematically controlling the pore architecture and a general strategy of fine-tuning the surface area by copolymerization of monomers with different "strut lengths".[2a–c] Controlling pore size systematically at less than 1 nm dimension is particularly challenging due to limited choice of molecular struts. We report here a new approach of synthesizing porous organic polymer (POP) with narrowly distributed PD between 0.7 to 0.9 nm and SSA > 1000 m^2 g^{-1} using an ethynyl trimerization reaction. Starting from four simple monomers **M1–M4** listed in Scheme 1, we successfully prepared a series of polyphenylenes with tunable diameters ranging from 0.7 nm to 0.9 nm. Simple aromatic framework and incremental variation of pore size with similar SSA make this group of polymers unique model materials for studying gas-adsorbent interaction with various gases, such as hydrogen, methane, *etc.*

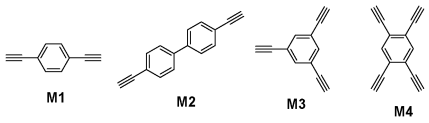

Scheme 1 Structure of the monomers **M1–M4**.

Using dicobalt octacarbonyl as a catalyst, the terminal ethynyl groups of the respective monomers were trimerized, and four polymers were readily obtained in quantitative yield. A representative polymerization to prepare polymer **POP-1** from **M1** is outlined in Scheme 2 (details about synthesis of other three polymers **POP-2**, **POP-3**, and **POP-4** from **M2**, **M3**, and **M4**, respectively, are shown in Scheme S1 in the Electronic Supplemental Information (ESI)).† While **M1** was purchased commercially, monomers **M2**, **M3** and **M4** were synthesized by coupling the aromatic bromides and trimethylsilylacetylene under Sonagarshira reaction conditions, followed by deprotection of the trimethylsilyl (TMS) groups. These monomers were designed in such a way that they could potentially form porous structures with different pore diameters and cross-linking density.

The structural properties of these polymers were characterized by Fourier transform infrared spectroscopy (FTIR) (See ESI).† The characteristic vibration band of alkynyl carbon-hydrogen at 3300 cm^{-1} is completely diminished for **POP-1** and **POP-2**, indicating the completion of the trimerization reaction; whereas this band is weakly observable for polymers **POP-3** and **POP-4**

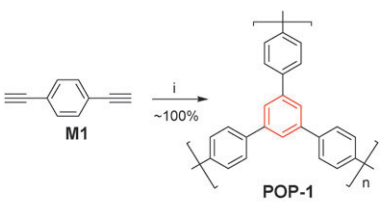

Scheme 2 Preparation of **POP-1** (benzene in red indicates one of the potential trimerization pathways from ethynyl groups).

[a] *Chemical Sciences & Engineering Division, Argonne National Laboratory, 9700 S. Cass Avenue, Argonne, IL 60439, USA. E-mail: djliu@anl.gov; Fax: +1 630 252 4176; Tel: +1 630 252 4511*
[b] *Materials Science Division, Argonne National Laboratory, 9700 S. Cass Avenue, Argonne, IL 60439, USA*
[c] *Department of Chemistry & The James Franck Institute, The University of Chicago, 929 E. 57th Street, Chicago, IL 60637, USA. E-mail: lupingyu@uchcicago.edu; Fax: +1 773 702 0805; Tel: +1 773 702 8698*

† Electronic supplementary information (ESI) available: Details on polymer synthesis, characterization, H_2 adsorption isotherm measurement and computational modeling. See DOI: 10.1039/c0cc00235f

due to the residual ethynyl groups, suggesting that even higher surface area maybe achievable should the trimerization be completed. The thermal gravimetric analysis (TGA) in air showed high thermal stability for polymers **POP-1**, **POP-2**, and **POP-3** with no sign of decomposition up to 360 °C. Polymer **POP-4** is also stable up to ~330 °C after an initial weight loss of about 10% due to the removal of residual moisture or air upon heating.

Surface properties of these polymers were characterized with nitrogen adsorption analysis at 77.3 K using a Micromeritics ASAP 2010 system. Nitrogen adsorption isotherms are shown in Fig. 1. The inset of Fig. 1 is the expanded plots at the low pressure region where nitrogen uptake is most sensitive to micropores (logarithmic pressure scale was used). The difference in nitrogen adsorption isotherms among these polymer samples are distinct. The inflection points of nitrogen uptake follow the sequence of **POP-2** < **POP-1** < **POP-4** < **POP-3**, suggesting their micropore diameters follow the same order. Fig. 2 shows the differential pore volume distributions as a function of pore width calculated with non-local density functional theory (NLDFT). Micropores are dominant for all four polymers. The inset in Fig. 2 represents an expanded view of pore size distribution from 0.7 to 0.9 nm. A similar differential pore volume distribution at slightly larger PDs was also found using Horváth-Kawazoe (H–K) method (Fig. S3 in ESI).†

A preliminary quantum chemical simulation of the polymer structures suggests that **POP-1** and **POP-2**, which form fewer bonds between monomers during the trimerization reaction

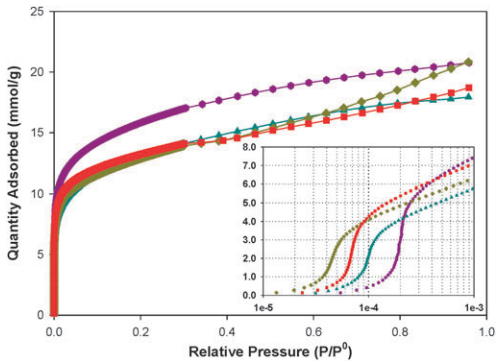

Fig. 1 Nitrogen adsorption isotherms measured at 77.3 K for polymers **POP-1** (square), **POP-2** (diamond), **POP-3** (hexagon), and **POP-4** (triangle).

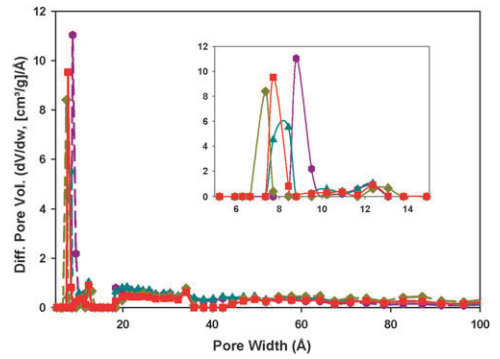

Fig. 2 Pore size distribution based on NLDFT calculation for **POP-1** (square), **POP-2** (diamond), **POP-3** (hexagon), and **POP-4** (triangle).

than **POP-3** and **POP-4**, have more structural flexibility. The phenylene and diphenylene units of the monomers **M1** and **M2** could rotate more freely than the phenylene units of **M3** and **M4**, which linked to three or four other monomers. More importantly, **POP-1** and **POP-2** tend to form relatively flexible structures through extending of **M1** or **M2**, which can stack and interpenetrate, thus reducing pore sizes. For **POP-3** and even more so for **POP-4**, a high strain among the monomers cause the crosslinking to extend three-dimensionally instead of just planarly, thus leading to a robust three-dimensional structure with less flexibility than **POP-1** and **POP-2**, suggesting a higher porosity. The strain arising due to the high density of ethynyl groups also results in the incompletion of the trimerization reaction, which was observed for **POP3** and **POP-4** experimentally. This correlates with the sequence of porosity **POP-2** ≤ **POP-1** < **POP-4** < **POP-3** found through N_2 adsorption analysis. All of the polymers have Brunauer-Emmet-Teller (BET) specific surface area (SSA) of more than 1000 $m^2\ g^{-1}$, with the highest value of 1246 $m^2\ g^{-1}$ for polymer **POP-3**. A summary of the surface areas using both BET model and Langmuir model, together with other structural properties are listed in Table 1.

Excess hydrogen adsorption capacities of these four polymers were measured with a modified Sievert isotherm apparatus.[4] Hydrogen adsorption/desorption isotherms were measured under four different temperatures for each polymer. Shown in Fig. 3 is a complete set of four isotherms for polymer **POP-3** with hydrogen uptakes up to 3 wt% obtained at 77 K and 60 bar (a summary of hydrogen adsorption capacities for **POP-3** and other polymers is listed in Table S1 in ESI).† Fig. 4 shows the heats of adsorption derived from the hydrogen adsorption isotherms at 195 K and 298 K, from which the initial adsorption energy can be calculated more accurately. **POP-4** and **POP-3** exhibited relatively higher initial heat of adsorption, ΔH_{ads}, around 9 kJ mol^{-1}, whereas **POP-1** and **POP-2** showed values of ΔH_{ads} near 7.5 kJ mol^{-1}. This observation offers little correlation between ΔH_{ads} and PDs obtained from N_2 adsorption isotherms. Instead, we found an interesting correlation between ΔH_{ads} and N_p where N_p represents the average number of phenyl groups connected to a benzene after trimerization. The N_p values for **POP-2** and **POP-1** of 2.3 and 2.5 are considerably lower than those for **POP-3** and **POP-4** of 3 and 3.5, respectively. Quantum chemical calculations at MP2/6-311++G(2d,2p)//MP2/6-31+G* level for H_2 adsorption on **M1**, **M3** and **M4** monomers simulating different arrangements of neighboring phenyl groups in the polymers resulted in binding energies of 5.1 kJ mol^{-1}, 5.5 kJ mol^{-1} and 6.0 kJ mol^{-1}, respectively. All structures were fully optimized, resulting in a vertical H_2 in the center of aromatic ring (see ESI for details).† Other phenyl groups adjacent to the H_2 could also contribute to the van der Waals interaction, particularly at low H_2 coverage. It is substantiated by calculations of the binding energies of H_2 to two monomers, which come out to be 10.6 kJ mol^{-1}, 12.6 kJ mol^{-1} and 12.9 kJ mol^{-1} for **M1**, **M3** and **M4**, respectively. Larger N_p leads to higher ΔH_{ads} as the order of **POP-4** > **POP-3** > **POP-1** ≥ **POP-2** we observed in Fig. 4 at low hydrogen coverage. Heat of adsorptions at higher coverage were also extrapolated from isotherms at 77 K and 87 K, the

Table 1 Surface properties of the polymers

	BET Surface Area/m^2 g^{-1}	Langmuir Surface Area/m^2 g^{-1}	Total Pore Volume/cm^3 g^{-1}[a]	Micropore Volume/cm^3 g^{-1}[a]	DFT Dominant Pore Diameter/nm[a]	H–K Dominant Pore Diameter/nm[b]
POP-1	1031	1387	0.641	0.378	0.77	0.83
POP-2	1013	1378	0.712	0.341	0.74	0.80
POP-3	1246	1515	0.729	0.448	0.88	0.90
POP-4	1033	1402	0.730	0.402	0.81	0.85

[a] Data calculated from nitrogen adsorption isotherm with NLDFT method. [b] Data calculated from nitrogen adsorption isotherm with H–K method.

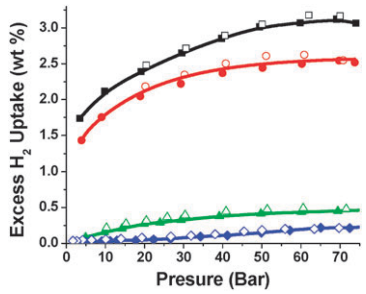

Fig. 3 Hydrogen adsorption (solid symbols)/desorption (open symbols) isotherms for polymer **POP-3** under 77 K (squares), 87 K (circles), 195 K (triangles), and room temperature (diamonds).

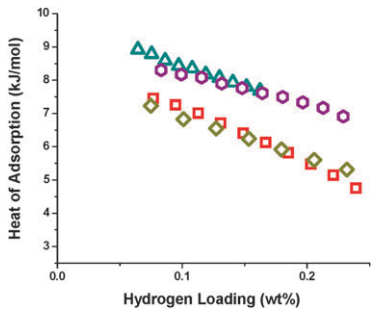

Fig. 4 Heat of adsorption at low coverage for **POP-1** (red square), **POP-2** (yellow diamond), **POP-3** (magenta hexagon), and **POP-4** (cyan triangle).

values of ΔH_{ads} at around 1.5 wt% hydrogen loading were in the range of 4.5–6.5 kJ mol^{-1}, and did not correlate with PD or N_p. This is somewhat expected since hydrogen adsorption is less sensitive to the surface structure at 77 K or 87 K as hydrogen loading increases.

We should point out that these POPs are generally considered amorphous with 3-dimensionally arranged network structures. The relatively higher ΔH_{ads} for **POP-3** and **POP-4** could also be due to the existence of hidden ultra-small pores resulting from higher number of trimerization sites, thus not accessible to N_2 during BET isotherm measurement.

In summary, four porous polymers with surface areas up to 1246 m^2 g^{-1} have been successfully synthesized from simple, aromatic ethynyl monomers. The polymeric pores are all narrowly distributed and fine-tuned with a dimension variability of less than 1 nm, close to the van der Waals diameters of various small gas molecules. Isosteric heat of adsorption measurement revealed that ΔH_{ads} is more sensitive to monomer structure than the pore size within the range of PD studied. Further investigation on hydrogen-polymer interaction in confined space at the molecular level using advanced characterization methods is underway.

This work was supported by the U.S. Department of Energy's Fuel Cell Technologies program under the Office of Energy Efficiency and Renewal Energy. The authors wish to thank Dr Shengqian Ma for his helpful discussion and experimental support from Mr Jose R. Regalbuto. Use of Argonne's LCRC computational resources is gratefully acknowledged.

Notes and references

1 (*a*) B. S. Ghanem, K. J. Msayib, N. B. McKeown, K. D. M. Harris, Z. Pan, P. M. Budd, A. Butler, J. Selbie, D. Book and A. Walton, *Chem. Commun.*, 2007, 67–69; (*b*) N. B. McKeown, B. Ghanem, K. J. Msayib, P. M. Budd, C. E. Tattershall, K. Mahmood, S. Tan, D. Book, H. Langmi and A. Walton, *Angew. Chem., Int. Ed.*, 2006, **45**, 1804–1807; (*c*) P. M. Budd, E. S. Elabas, B. S. Ghanem, S. Makhseed, N. B. Mckeown, K. J. Msayib, C. E. Tattershall and D. Wang, *Adv. Mater.*, 2004, **16**, 456–459; (*d*) S. Makhseed and J. Samuel, *Chem. Commun.*, 2008, 4342–4344; (*e*) N. Du, G. P. Robertson, J. Song, I. Pinnau, S. Thomas and M. D. Guiver, *Macromolecules*, 2008, **41**, 9656–9662.

2 (*a*) J.-X. Jiang, F. Su, A. Trewin, C. D. Wood, H. Niu, J. T. A. Jones, Y. Z. Khimyak and A. I. Cooper, *J. Am. Chem. Soc.*, 2008, **130**, 7710–7720; (*b*) J.-X. Jiang, F. Su, A. Trewin, C. D. Wood, N. L. Campbell, H. Niu, C. Dickinson, A. Y. Ganin, M. J. Rosseinsky, Y. Z. Khimyak and A. I. Cooper, *Angew. Chem., Int. Ed.*, 2007, **46**, 8574–8578; (*c*) J.-X. Jiang, A. Trewin, F. Su, C. D. Wood, H. Niu, J. T. A. Jones, Y. Z. Khimyak and A. I. Cooper, *Macromolecules*, 2009, **42**, 2658–2666; (*d*) E. Stöckel, X. Wu, A. Trewin, C. D. Wood, R. Clowes, N. L. Campbell, J. T. A. Jones, Y. Z. Khimyak, D. J. Adams and A. I. Cooper, *Chem. Commun.*, 2009, 212–214.

3 (*a*) C. D. Wood, B. Tan, A. Trewin, H. Niu, D. Bradshaw, M. J. Rosseinsky, Y. Z. Khimyak, N. L. Campbell, R. Kirk, E. Stockel and A. I. Cooper, *Chem. Mater.*, 2007, **19**, 2034–2048; (*b*) J.-Y. Lee, C. D. Wood, D. Bradshaw, M. J. Rosseinsky and A. I. Cooper, *Chem. Commun.*, 2006, 2670–2672.

4 S. Yuan, S. Kirklin, B. Dorney, D.-J. Liu and L. Yu, *Macromolecules*, 2009, **42**, 1554–1559.

5 M. Rose, W. Bohlmann, M. Sabo and S. Kaskel, *Chem. Commun.*, 2008, 2462–2464.

6 (*a*) J. Weber, M. Antonietti and A. Thomas, *Macromolecules*, 2008, **41**, 2880–2885; (*b*) J. Schmidt, J. Weber, J. D. Epping, M. Antonietti and A. Thormas, *Adv. Mater.*, 2009, **21**, 702–705; (*c*) J. Weber and A. Thomas, *J. Am. Chem. Soc.*, 2008, **130**, 6334–6335; (*d*) J. Weber, Q. Su, M. Antonietti and A. Thomas, *Macromol. Rapid Commun.*, 2007, **28**, 1871–1876.

7 F. J. Uribe-Romo, J. R. Hunt, H. Furukawa, C. Klock, M. O'Keeffe and O. M. Yaghi, *J. Am. Chem. Soc.*, 2009, **131**, 4570–4571.

8 J. Schmidt, M. Werner and A. Thomas, *Macromolecules*, 2009, **42**, 4426–4429.

9 (*a*) J. Germain, J. Hradil, J. M. J. Frechet and F. Svec, *Chem. Mater.*, 2006, **18**, 4430–4435; (*b*) J. Germain, F. Svec and J. M. J. Frechet, *Chem. Mater.*, 2008, **20**, 7069–7076.